Editors' Suggestion

Determination of Spin-Parity Quantum Numbers of $X(2370)$ as 0^{-+} from $J/\psi \to \gamma K_S^0 K_S^0 \eta'$

M. Ablikim *et al.*[*]
(BESIII Collaboration)

(Received 8 December 2023; revised 5 March 2024; accepted 28 March 2024; published 2 May 2024)

Based on $(10087 \pm 44) \times 10^6$ J/ψ events collected with the BESIII detector, a partial wave analysis of the decay $J/\psi \to \gamma K_S^0 K_S^0 \eta'$ is performed. The mass and width of the $X(2370)$ are measured to be $2395 \pm 11(\mathrm{stat})^{+26}_{-94}(\mathrm{syst})$ MeV$/c^2$ and $188^{+18}_{-17}(\mathrm{stat})^{+124}_{-33}(\mathrm{syst})$ MeV, respectively. The corresponding product branching fraction is $\mathcal{B}[J/\psi \to \gamma X(2370)] \times \mathcal{B}[X(2370) \to f_0(980)\eta'] \times \mathcal{B}[f_0(980) \to K_S^0 K_S^0] = (1.31 \pm 0.22(\mathrm{stat})^{+2.85}_{-0.84}(\mathrm{syst})) \times 10^{-5}$. The statistical significance of the $X(2370)$ is greater than 11.7σ and the spin parity is determined to be 0^{-+} for the first time. The measured mass and spin parity of the $X(2370)$ are consistent with the predictions of the lightest pseudoscalar glueball.

DOI: 10.1103/PhysRevLett.132.181901

The non-Abelian property of quantum chromodynamics (QCD) permits the existence of new types of hadrons, such as glueballs, hybrids, and multiquark states, which are beyond conventional mesons and baryons in the constituent quark model [1–3]. In particular, the glueball is a unique particle formed via the interaction among gauge boson particles. Lattice quantum chromodynamics (LQCD) predicts that the ground state of a pseudoscalar glueball has a mass around 2.3–2.6 GeV$/c^2$ [4–8]. The radiative decay of the J/ψ meson is a gluon-rich process and is therefore regarded as an ideal place for searching and studying glueballs [9,10].

A $\pi^+\pi^-\eta'$ resonance, the $X(2370)$, was observed in $J/\psi \to \gamma\pi^+\pi^-\eta'$ with a statistical significance greater than 6.4σ in the BESIII experiment [11]. It was further observed from the combined measurement of $J/\psi \to \gamma K^+K^-\eta'$ and $J/\psi \to \gamma K_S^0 K_S^0 \eta'$ with a statistical significance of 8.3σ by BESIII [12]. This experimental observation stimulated a number of theoretical speculations [13–17] for its nature. Among them, one of the intriguing explanations is a pseudoscalar glueball [8,18–20]. A high-statistics J/ψ data sample collected with BESIII provides an opportunity to further investigate the properties of the $X(2370)$ and helps to understand the dynamics of QCD.

To understand the nature of the $X(2370)$, it is crucial to measure its quantum numbers J^{PC} and the decay modes. In contrast to $J/\psi \to \gamma K^+K^-\eta'$, there is no background contamination for $J/\psi \to \gamma K_S^0 K_S^0 \eta'$ from $J/\psi \to \pi^0 K_S^0 K_S^0 \eta'$ and $J/\psi \to K_S^0 K_S^0 \eta'$, which are forbidden by exchange symmetry and CP conservation. Therefore, the $J/\psi \to \gamma K_S^0 K_S^0 \eta'$ decay provides a clean environment for its J^{PC} measurement with minimal background modeling uncertainties. In this Letter, we report the first spin-parity determination of the $X(2370)$ in the decay $J/\psi \to \gamma K_S^0 K_S^0 \eta'$, where the K_S^0 decays to $\pi^+\pi^-$ and the η' decays to the two most dominant channels $\eta' \to \gamma\pi^+\pi^-$ and $\eta' \to \eta\pi^+\pi^-(\eta \to \gamma\gamma)$. The analysis is based on $(10087 \pm 44) \times 10^6$ J/ψ events [21] collected in the BESIII detector [22].

A detailed description of the design and performance of the BESIII detector can be found in Ref. [22]. Simulated samples produced with a GEANT4-based [23] Monte Carlo (MC) package, which includes the geometric description of the BESIII detector [24] and the detector response, are used for the optimization of event selection criteria and detection efficiency determination. Signal MC samples for the process $J/\psi \to \gamma K_S^0 K_S^0 \eta'$ with the subsequent decays $K_S^0 \to \pi^+\pi^-$, $\eta' \to \pi^+\pi^-\eta$, and $\eta \to \gamma\gamma$ are generated uniformly in phase space. A special generator takes $\rho - \omega$ interference and box anomaly into account [25] in the process of $\eta' \to \gamma\pi^+\pi^-$.

Charged tracks reconstructed from the multilayer drift chamber (MDC) are required to be within the polar angle range $|\cos\theta| < 0.93$, where θ is defined with respect to the z axis, which is the symmetry axis of the MDC. The distance of closest approach to the interaction point for charged tracks (excluding those from K_S^0 decays) must be less than 10 cm along the z axis and less than 1 cm in the transverse plane. All charged tracks are assumed to be pions. To reconstruct K_S^0 candidates, the tracks of each $\pi^+\pi^-$ pair are fitted to a secondary vertex. To suppress background events, all K_S^0 candidates are required to satisfy $|M_{\pi^+\pi^-} - m_{K_S^0}| < 9$ MeV$/c^2$, where $m_{K_S^0}$ is the known mass of K_S^0 [26]. To further suppress background, the

[*]Full author list given at the end of the Letter.

decay length of K_S^0 candidate, i.e., the distance between the average position of the e^+e^- collisions and the decay vertex of K_S^0, is required to be greater than twice the vertex resolution. With these selections, the miscombination of K_S^0 reconstruction is significantly suppressed to be less than 0.1%. The reconstructed K_S^0 candidates are used as an input for the subsequent kinematic fit.

Photon candidates are identified using showers in the electromagnetic calorimeter (EMC). The deposited energy of each shower are required to have at least 100 MeV in the barrel region ($|\cos\theta| < 0.80$) and the end cap region ($0.86 < |\cos\theta| < 0.92$). To exclude showers from charged tracks, the angle between the shower position and the charged tracks extrapolated to the EMC must be greater than 10°. The difference between the EMC time and the event start time is required to be within [0, 700] ns in order to suppress electronic noise and energy deposits unrelated to the event.

For the $J/\psi \to \gamma K_S^0 K_S^0 \eta'$, $\eta' \to \gamma\pi^+\pi^-$ channel, each candidate event is required to have at least three positively charged tracks, at least three negatively charged tracks and two photons. A four-constraint (4C) kinematic fit under the $J/\psi \to \gamma\gamma K_S^0 K_S^0 \pi^+\pi^-$ hypothesis is performed by enforcing energy-momentum conservation. If there is more than one $\gamma\gamma K_S^0 K_S^0 \pi^+\pi^-$ combination, the one with the smallest χ^2_{4C} is chosen. The resulting χ^2_{4C} is required to be less than 40. The η' candidates are required to have the invariant mass satisfying $|M_{\gamma\pi^+\pi^-} - m_{\eta'}| < 15$ MeV$/c^2$, where $m_{\eta'}$ is the known mass of η' [26]. If there is more than one $\gamma\pi^+\pi^-$ combination, the one with the minimum $|M_{\gamma\pi^+\pi^-} - m_{\eta'}|$ is selected. The $\pi^+\pi^-$ (from η') invariant mass is required to be in the ρ mass region, $0.55 < M_{\pi^+\pi^-} < 0.90$ GeV$/c^2$. To suppress background events containing a π^0 or η, events with $|M_{\gamma\gamma} - m_{\pi^0}| < 20$ MeV$/c^2$ or $|M_{\gamma\gamma} - m_\eta| < 30$ MeV$/c^2$ are rejected, where m_{π^0} and m_η are the known masses of π^0 and η, respectively [26].

For the $J/\psi \to \gamma K_S^0 K_S^0 \eta'$, $\eta' \to \pi^+\pi^-\eta$, $\eta \to \gamma\gamma$ channel, each candidate event is required to have at least three positively charged tracks, at least three negatively charged tracks and three photons. A 4C kinematic fit is performed under the $J/\psi \to \gamma\gamma\gamma K_S^0 K_S^0 \pi^+\pi^-$ hypothesis and the combination with the smallest χ^2_{4C} is chosen if more than one combination is found. In order to reduce background and to improve the mass resolution, a five-constraint (5C) kinematic fit is performed to further constrain the invariant mass of the two photons to m_η. Among three $\gamma\gamma$ combinations, the one with the smallest χ^2_{5C} is chosen, and $\chi^2_{5C} < 50$ is required. The η' candidates must satisfy $|M_{\pi^+\pi^-\eta} - m_{\eta'}| < 10$ MeV$/c^2$. To suppress background events containing a π^0, events with $|M_{\gamma\gamma} - m_{\pi^0}| < 20$ MeV$/c^2$ are rejected, where the photon pairs are all possible combinations of the radiative photon and photons from η.

All the above selection criteria aim to improve the signal extraction efficiency and signal-to-noise ratio. The mass windows for peaking signals of K_S^0 and η' correspond to approximately 3 standard deviations to their respective known masses [26]. Others are determined by optimizing the figure of merit (FOM) $\epsilon_S/\sqrt{N_{\rm data}}$, where ϵ_S is signal efficiency with simulation MC sample, and $N_{\rm data}$ is the final selected event number in data. With above criteria, the event numbers of final selected candidates are 4046 and 1395 for the $\eta' \to \gamma\pi^+\pi^-$ channel and the $\eta' \to \pi^+\pi^-\eta$ channel, respectively.

No significant peaking background contribution has been found in the measured invariant mass spectra. The remaining background component is from non-η' processes, which are estimated from the η' mass sideband regions of $20 < |M_{\gamma\pi^+\pi^-} - m_{\eta'}| < 30$ MeV$/c^2$ and $30 < |M_{\pi^+\pi^-\eta} - m_{\eta'}| < 40$ MeV$/c^2$. The corresponding background fractions are 6.8% and 1.8% for the two channels, respectively.

Figure 1 shows the mass distributions with the above selection criteria for the $\eta' \to \gamma\pi^+\pi^-$ and $\eta' \to \pi^+\pi^-\eta$ channels. Similar structures are observed in the two channels. The two-dimensional distributions of $M_{K_S^0K_S^0}$ versus $M_{K_S^0K_S^0\eta'}$ indicate a strong enhancement near the

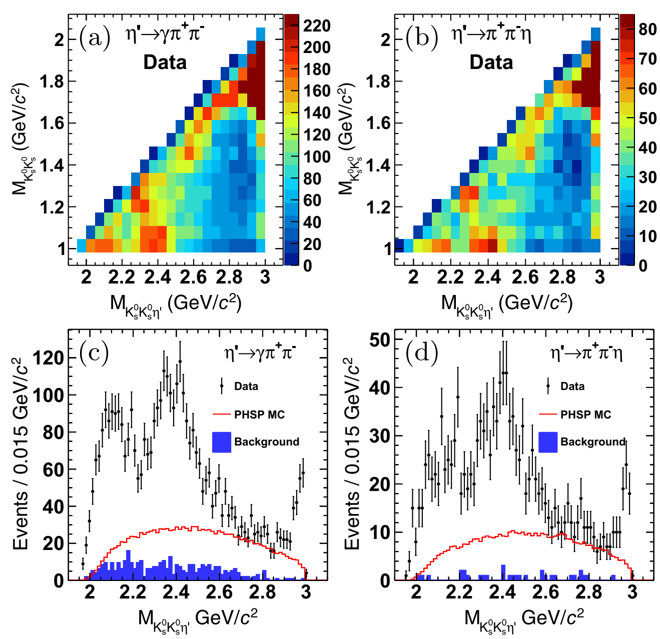

FIG. 1. Invariant mass distributions of the selected events: (a) and (b) The two-dimensional distributions of $M_{K_S^0K_S^0}$ versus $M_{K_S^0K_S^0\eta'}$ for the $\eta' \to \gamma\pi^+\pi^-$ and $\eta' \to \pi^+\pi^-\eta$ channels, respectively. (c) and (d) The $K_S^0K_S^0\eta'$ invariant mass distributions with the requirement $M_{K_S^0K_S^0} < 1.1$ GeV$/c^2$ for $\eta' \to \gamma\pi^+\pi^-$ and $\eta' \to \pi^+\pi^-\eta$ channels, respectively. The dots with error bars are data. The shaded histograms are the non-η' backgrounds estimated by the η' sideband. The solid lines are phase space (PHSP) MC events with arbitrary normalization.

$K_S^0K_S^0$ mass threshold from the $f_0(980)$ and a clear connection between the $f_0(980)$ and the structure around 2.4 GeV$/c^2$, $X(2370)$, in the invariant mass spectra of $K_S^0K_S^0\eta'$. By requiring $M_{K_S^0K_S^0} < 1.1$ GeV$/c^2$, the structure around 2.4 GeV$/c^2$ becomes much more prominent in the $K_S^0K_S^0\eta'$ mass spectrum. In addition, there is a clear signature from the η_c.

A partial wave analysis (PWA) is performed to investigate the properties of the $X(2370)$. To reduce complexities from additional intermediate processes, events satisfying $M_{K_S^0K_S^0} < 1.1$ GeV$/c^2$ are used. The K_S^0 and η' momenta are constrained to their known masses, respectively. The signal amplitudes are constructed with the covariant tensor formalism [27] and parametrized as quasi-sequential two-body decays: $J/\psi \to \gamma X$, $X \to Y\eta'$ or $X \to ZK_S^0$, where Y and Z represent $K_S^0K_S^0$ and $K_S^0\eta'$ isobars, respectively. Because of the parity conservation, the possible J^{PC} of $K_S^0K_S^0\eta'$ system (X) are 0^{-+}, 1^{++}, 2^{++}, 2^{-+}, etc. In this Letter, given the suppression of phase space factor, only spin $J < 3$ states of the X and possible S-wave or P-wave and D-wave decays of intermediate states are considered. An unbinned maximum likelihood fit is performed on the combined data of the two η' decay modes. The non-η' background contribution is taken into account in the fit via the subtraction of the negative log-likelihood values with the events estimated from the η' mass sideband region.

The optimal PWA fit shows that data can be well described with a process combination of the decay of $f_0(980)\eta'$ from the resonances of the $X(1835)$, $X(2370)$, η_c and a broad 0^{-+} structure denoted as $X(2800)$, and the nonresonance components of $(K_S^0K_S^0)_S\eta'$ and $(K_S^0K_S^0)_D\eta'$ for the S wave and D wave in the $K_S^0K_S^0$ system, respectively. The $X(1835)$, $X(2370)$, and $X(2800)$ are described by nonrelativistic Breit-Wigner (BW) functions, where the intrinsic widths are not energy dependent. The masses and widths of the $X(1835)$ and η_c are fixed to previous measurements [26,28]. The masses and widths of the $X(2370)$ and $X(2800)$ are floated in the PWA fit. The mass line shape of $f_0(980)$ is parametrized by the Flatté formula [29] with the BESII measurement [30]. The J^{PC} of the $X(2370)$ and $X(2800)$ are assigned to be 0^{-+}. The statistical significance of the $X(2370)$ is greater than 11.7σ, which is determined from the changes of log-likelihood value and degrees of freedom in the PWA fits with and without the signal hypotheses for every systematic variation. The mass, width, and product branching fraction of $X(2370)$ are measured to be $2395 \pm 11(\mathrm{stat})$ MeV$/c^2$, $188^{+18}_{-17}(\mathrm{stat})$ MeV$/c^2$ and $\mathcal{B}[J/\psi \to \gamma X(2370)] \times \mathcal{B}[X(2370) \to f_0(980)\eta'] \times \mathcal{B}[f_0(980) \to K_S^0K_S^0] = (1.31 \pm 0.22(\mathrm{stat})) \times 10^{-5}$, respectively. Figure 2 provides the comparisons of the mass and angular distributions between data and PWA fit projections, as well as the individual contributions from each component. The χ^2/n_{bin} value is

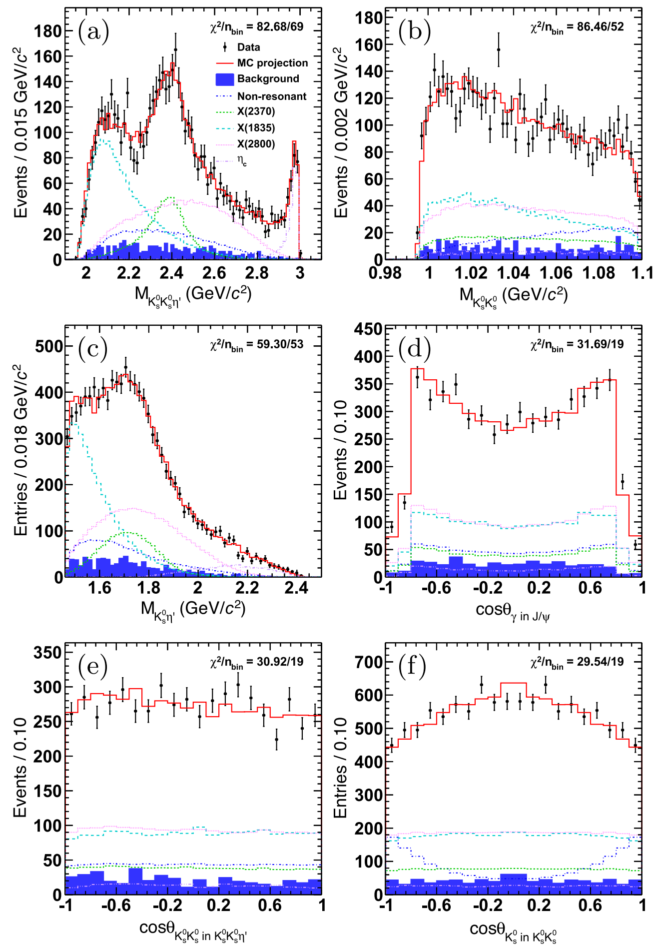

FIG. 2. Comparisons between data (with two η' decay modes combined) and PWA fit projections: (a),(b), and (c) The invariant mass distributions of $K_S^0K_S^0\eta'$, $K_S^0K_S^0$, and $K_S^0\eta$ (two entries for one event), respectively. (d),(e) and (f) are the angular distributions of $\cos\theta$, where θ is the polar angle of (d) γ in the J/ψ rest system; (e) $K_S^0K_S^0$ in the $K_S^0K_S^0\eta'$ rest system; and (f) K_S^0 in the $K_S^0K_S^0$ rest system (two entries for one event). The dots with error bars are data. The solid red histograms are the PWA total projections. The shaded histograms are the non-η' backgrounds described by the η' sideband. The dash-dotted blue, short dashed green, long dashed cyan, dotted magenta, and dash-dot-dotted violet show the contributions of the nonresonant contribution, $X(2370)$, $X(1835)$, $X(2800)$ and η_c, respectively.

displayed on each figure to demonstrate the goodness of fit. A broad 0^{-+} structure is needed in the optimal PWA fit to describe the effective contributions from possible high-mass resonances such as $X(2600)$ [31] and the tail of η_c line shape, which is denoted as $X(2800)$ (with a mass of 2799 and a width of 660 MeV$/c^2$). The $X(2800)$ have been checked with various alternative PWA fits. For example, if the η_c line shape is parametrized without a damping factor [32], the significance of $X(2800)$ is reduced to 3.1σ. If the $X(2800)$ is not included in the PWA, the spin parity of $X(2370)$ remains to be 0^{-+} with a significance greater than 10.1σ. The significance of 0^{-+} over other alternative J^{PC} is determined from the changes of log-likelihood value and degrees of freedom in PWA fits. The impacts of the $X(2800)$ on the mass, width, and product branching fraction of the $X(2370)$ are included in the systematic uncertainties.

Variations of the PWA fit including the J^{PC} and decay mode for each component are tested. Possible decay modes [$f_0(1500)\eta'$, $f_2(1270)\eta'$, $K^*(1410)K_S^0$, $K_0^*(1430)K_S^0$, $K_2^*(1430)K_S^0$, $K^*(1680)K_S^0$, $(K_S^0K_S^0)_S\eta'$, $(K_S^0K_S^0)_D\eta'$, $(K_S^0\eta')_PK_S^0$, $(K_S^0\eta')_DK_S^0$] are evaluated via different process combinations. All additional decay modes have significances lower than 3σ. The contributions from additional resonances are also evaluated, including the $\eta(1760)$, $\eta(2225)$, $\eta_2(1870)$, $X(2120)$ [11], and $X(2600)$ [31]. All the significances of each contribution are measured to be less than 3σ, except the $X(2600)$. The significance of the process of $X(2600) \to f_0(980)\eta'$ is 4.2σ. This process is not included in the optimal solution, but the possible contribution of this process is taken into account as a source of systematic uncertainties. The scan results yield no evidence for extra intermediate states. For the spin-parity determination of the $X(2370)$, the 0^{-+} assignment fit is better than that for 1^{++} or 2^{-+} assignments with significances that are greater than 10.8σ or 9.8σ, respectively. The significances are evaluated with the consideration of all systematic uncertainty variations as described below.

Systematic uncertainty associated with the PWA affects both the branching fraction measurement and the resonance parameters, including the background contribution, $f_0(980)$ mass line shape, the $X(1835)$ mass line shape, η_c mass line shape, BW formula, additional resonances and description of the broad 0^{-+} structure. The uncertainty due to the background contribution is estimated using different background normalization factors and different η' sideband regions. The $f_0(980)$ mass line shape is varied by changing the mass and coupling constants in the *Flatté* formula to other experimental measurements [33]. Uncertainty from the $X(1835)$ mass line shape includes the variation with 1 standard deviation of the mass and width measurement [28] and the alternative parametrization of the anomalous line shape near the $p\bar{p}$ mass threshold [34]. Uncertainty from the η_c mass line shape is estimated by turning off the damping factor [32]. Uncertainty arising from the BW parametrization is estimated by replacing the constant width with a mass-dependence width [35]. The impact from possible additional resonances is estimated by including the contributions of $X(2120)$ and $X(2600)$ to the PWA fit. The broad 0^{-+} structure is described with the $X(2800)$ in the optimal PWA fit and has been checked with various PWA fits including replacing the $X(2800)$ with a nonresonance component of $f_0(980)\eta'$, removing the $X(2800)$ and adding a non-resonance component of $f_0(980)\eta'$ for the exclusion of the damping factor for the η_c. The envelope of those variations is assigned as the final uncertainty from the description of the broad 0^{-+} structure. This is the dominant systematic uncertainty source for the measurements of mass, width, and product branching fraction of the $X(2370)$.

TABLE I. Systematic uncertainties on the measurements of mass, width, and product branching fraction of the $X(2370)$.

Sources	ΔM (MeV/c^2)	$\Delta\Gamma$ (MeV)	$\Delta\mathcal{B}/\mathcal{B}(\%)$
Event selection	⋯	⋯	±4.8
Background estimation	$+2$	$^{+4}_{-4}$	$^{+3.7}_{-5.1}$
$f_0(980)$ parametrization	-6	$+7$	±5.3
X(1835) parametrization	$^{+15}_{-12}$	$^{+24}_{-11}$	$^{+20.2}_{-8.3}$
η_c parametrization	-13	-8	-14.5
Breit-Wigner formula	-1	$+6$	-8.3
Broad 0^{-+} structure	-88	$^{+111}_{-21}$	$^{+211.8}_{-56.5}$
Additional resonances	$^{+22}_{-25}$	$^{+48}_{-21}$	$^{+41.9}_{-20.8}$
Total	$^{+26}_{-94}$	$^{+124}_{-33}$	$^{+217.0}_{-63.7}$

Additional systematic uncertainty associated with the event selection, including tracking efficiency [36], photon selection efficiency [37], kinematic fit [38], K_S^0 reconstruction [39], the branching fractions of $K_S^0 \to \pi^+\pi^-$, $\eta' \to \pi^+\pi^-\eta$, $\eta' \to \gamma\pi^+\pi^-$ and $\eta \to \gamma\gamma$ [26], and the total number of J/ψ events [21], has been estimated to be $\pm4.8\%$ for the measurement of product branching fraction. All studied systematic uncertainty sources and their contributions are summarized in Table I and are treated independently. Total systematic uncertainties on the mass and width of the $X(2370)$ are $^{+26}_{-94}$ MeV/c^2 and $^{+124}_{-33}$ MeV, respectively, and total relative systematic uncertainty on the corresponding product branching fraction is $^{+217.0}_{-63.7}\%$.

In summary, a PWA of $J/\psi \to \gamma K_S^0K_S^0\eta'$ has been performed in the full $K_S^0K_S^0\eta'$ invariant mass range with the requirement of $M_{K_S^0K_S^0} < 1.1$ GeV/c^2. The PWA fit indicates a contribution from $X(2370) \to K_S^0K_S^0\eta'$ with a statistical significance greater than 14σ. The mass and width of the $X(2370)$ are measured to be $2395 \pm 11(\mathrm{stat})^{+26}_{-94}(\mathrm{syst})$ MeV/c^2 and $188^{+18}_{-17}(\mathrm{stat})^{+124}_{-33}(\mathrm{syst})$ MeV, respectively. These results agree with the previous measurements from $J/\psi \to \gamma\pi^+\pi^-\eta'$ [11] and $J/\psi \to \gamma K\bar{K}\eta'$ [12]. The corresponding product branching fraction is $\mathcal{B}[J/\psi \to \gamma X(2370)] \times \mathcal{B}[X(2370) \to f_0(980)\eta'] \times \mathcal{B}[f_0(980) \to K_S^0K_S^0] = (1.31 \pm 0.22(\mathrm{stat})^{+2.85}_{-0.84}(\mathrm{syst})) \times 10^{-5}$. The spin parity of the $X(2370)$ is determined to be 0^{-+} for the first time. The measured mass of $X(2370)$ is in a good agreement with the mass prediction of the lightest pseudoscalar glueball, which is expected to be (2.395 ± 0.014) GeV/c^2 from latest LQCD calculations [8].

The BESIII Collaboration thanks the staff of BEPCII and the IHEP computing center for their strong support. This work is supported in part by the National Key R&D Program of China under Contracts No. 2020YFA0406300 and No. 2020YFA0406400; National Natural Science Foundation of China (NSFC) under Contracts No. 11635010, No. 11735014, No. 11835012, No. 11935015, No. 11935016, No. 11935018, No. 11961141012, No. 12025502, No. 12035009, No. 12035013, No. 12061131003, No. 12192260, No. 12192261, No. 12192262, No. 12192263, No. 12192264, No. 12192265, No. 12221005, No. 12225509, No. 12235017; the Chinese Academy of Sciences (CAS) Large-Scale Scientific Facility Program; the CAS Center for Excellence in Particle Physics (CCEPP); Joint Large-Scale Scientific Facility Funds of the NSFC and CAS under Contract No. U1832207; CAS Key Research Program of Frontier Sciences under Contracts No. QYZDJ-SSW-SLH003 and No. QYZDJ-SSW-SLH040; 100 Talents Program of CAS; The Institute of Nuclear and Particle Physics (INPAC) and Shanghai Key Laboratory for Particle Physics and Cosmology; European Union's Horizon 2020 research and innovation programme under Marie Sklodowska-Curie grant agreement under Contract No. 894790; German Research Foundation DFG under Contracts No. 455635585, Collaborative Research Center CRC 1044, FOR5327, GRK 2149; Istituto Nazionale di Fisica Nucleare, Italy; Ministry of Development of Turkey under Contract No. DPT2006K-120470; National Research Foundation of Korea under Contract No. NRF-2022R1A2C1092335; National Science and Technology fund of Mongolia; National Science Research and Innovation Fund (NSRF) via the Program Management Unit for Human Resources & Institutional Development, Research and Innovation of Thailand under Contract No. B16F640076; Polish National Science Centre under Contract No. 2019/35/O/ST2/02907; The Swedish Research Council; U.S. Department of Energy under Contract No. DE-FG02-05ER41374.

[1] C. Amsler and N. A. Törnqvist, Phys. Rep. **389**, 61 (2004).
[2] E. Klempt and A. Zaitsev, Phys. Rep. **454**, 1 (2007).
[3] V. Crede and C. Meyer, Prog. Part. Nucl. Phys. **63**, 74 (2009).
[4] G. S. Bali, K. Schilling, A. Hulsebos, A. C. Irving, C. Michael, and P. W. Stephenson (UKQCD Collaboration), Phys. Lett. B **309**, 378 (1993).
[5] C. J. Morningstar and M. J. Peardon, Phys. Rev. D **60**, 034509 (1999).
[6] Y. Chen *et al.*, Phys. Rev. D **73**, 014516 (2006).
[7] E. Gregory, A. Irving, B. Lucini, C. McNeile, A. Rago, C. Richards, and E. Rinaldi, J. High Energy Phys. 10 (2012) 170.
[8] L.-C. Gui, J.-M. Dong, Y. Chen, and Y.-B. Yang, Phys. Rev. D **100**, 054511 (2019).
[9] M. B. Çakír and G. R. Farrar, Phys. Rev. D **50**, 3268 (1994).
[10] F. E. Close, G. R. Farrar, and Z. Li, Phys. Rev. D **55**, 5749 (1997).
[11] M. Ablikim *et al.* (BESIII Collaboration), Phys. Rev. Lett. **106**, 072002 (2011).
[12] M. Ablikim *et al.* (BESIII Collaboration), Eur. Phys. J. C **80**, 746 (2020).
[13] J.-S. Yu, Z.-F. Sun, X. Liu, and Q. Zhao, Phys. Rev. D **83**, 114007 (2011).
[14] C. Deng, J. Ping, Y. Yang, and F. Wang, Phys. Rev. D **86**, 014008 (2012).
[15] B.-D. Wan, S.-Q. Zhang, and C.-F. Qiao, Phys. Rev. D **105**, 014016 (2022).
[16] L.-M. Wang, Q.-S. Zhou, C.-Q. Pang, and X. Liu, Phys. Rev. D **102**, 114034 (2020).
[17] N. Su and H.-X. Chen, Phys. Rev. D **106**, 014023 (2022).
[18] J.-F. Liu, G.-J. Ding, and M.-L. Yan, Phys. Rev. D **82**, 074026 (2010).
[19] W. I. Eshraim, S. Janowski, F. Giacosa, and D. H. Rischke, Phys. Rev. D **87**, 054036 (2013).
[20] R. Zhang, W. Sun, Y. Chen, M. Gong, L.-C. Gui, and Z. Liu, Phys. Lett. B **827**, 136960 (2022).
[21] M. Ablikim *et al.* (BESIII Collaboration), Chin. Phys. C **46**, 074001 (2022).
[22] M. Ablikim *et al.* (BESIII Collaboration), Nucl. Instrum. Methods Phys. Res., Sect. A **614**, 345 (2010).
[23] S. Agostinelli *et al.*, Nucl. Instrum. Methods Phys. Res., Sect. A **506**, 250 (2003).
[24] K. X. Huang, Z.-J. Li, Z. Qian, J. Zhu, H.-Y. Li, Y.-M. Zhang, S.-S. Sun, and Z.-Y. You, Nucl. Sci. Tech. **33**, 142 (2022).
[25] M. Ablikim *et al.* (BESIII Collaboration), Phys. Rev. Lett. **120**, 242003 (2018).
[26] R. L. Workman *et al.* (Particle Data Group), Prog. Theor. Exp. Phys. **2022**, 083C01 (2022).
[27] B.-S. Zou and D. Bugg, Eur. Phys. J. A **16**, 537 (2003).
[28] M. Ablikim *et al.* (BESIII Collaboration), Phys. Rev. Lett. **115**, 091803 (2015).
[29] S. M. Flatte, Phys. Lett. **63B**, 224 (1976).
[30] M. Ablikim *et al.* (BES Collaboration), Phys. Lett. B **607**, 243 (2005).
[31] M. Ablikim *et al.* (BESIII Collaboration), Phys. Rev. Lett. **129**, 042001 (2022).
[32] M. Ablikim *et al.* (BESIII Collaboration), Phys. Rev. D **100**, 052012 (2019).
[33] R. Aaij *et al.* (LHCb Collaboration), Phys. Rev. D **86**, 052006 (2012).
[34] M. Ablikim *et al.* (BESIII Collaboration), Phys. Rev. Lett. **117**, 042002 (2016).
[35] M. Ablikim *et al.* (BESIII Collaboration), Phys. Rev. D **104**, 052006 (2021).
[36] M. Ablikim *et al.* (BESIII Collaboration), Phys. Rev. D **85**, 092012 (2012).
[37] M. Ablikim *et al.* (BESIII Collaboration), Phys. Rev. D **81**, 052005 (2010).
[38] M. Ablikim *et al.* (BESIII Collaboration), Phys. Rev. D **87**, 012002 (2013).
[39] M. Ablikim *et al.* (BESIII Collaboration), Phys. Rev. D **109**, 012006 (2024).

M. Ablikim,[1] M. N. Achasov,[4,b] P. Adlarson,[75] X. C. Ai,[80] R. Aliberti,[35] A. Amoroso,[74a,74c] M. R. An,[39] Q. An,[71,58] Y. Bai,[57] O. Bakina,[36] I. Balossino,[29a] Y. Ban,[46,g] H.-R. Bao,[63] V. Batozskaya,[1,44] K. Begzsuren,[32] N. Berger,[35] M. Berlowski,[44] M. Bertani,[28a] D. Bettoni,[29a] F. Bianchi,[74a,74c] E. Bianco,[74a,74c] A. Bortone,[74a,74c] I. Boyko,[36] R. A. Briere,[5] A. Brueggemann,[68] H. Cai,[76] X. Cai,[1,58] A. Calcaterra,[28a] G. F. Cao,[1,63] N. Cao,[1,63] S. A. Cetin,[62a] J. F. Chang,[1,58] W. L. Chang,[1,63] G. R. Che,[43] G. Chelkov,[36,a] C. Chen,[43] Chao Chen,[55] G. Chen,[1] H. S. Chen,[1,63] M. L. Chen,[1,58,63] S. J. Chen,[42] S. L. Chen,[45] S. M. Chen,[61] T. Chen,[1,63] X. R. Chen,[31,63] X. T. Chen,[1,63] Y. B. Chen,[1,58] Y. Q. Chen,[34] Z. J. Chen,[25,h] S. K. Choi,[10] X. Chu,[43] G. Cibinetto,[29a] S. C. Coen,[3] F. Cossio,[74c] J. J. Cui,[50] H. L. Dai,[1,58] J. P. Dai,[78] A. Dbeyssi,[18] R. E. de Boer,[3] D. Dedovich,[36] Z. Y. Deng,[1] A. Denig,[35] I. Denysenko,[36] M. Destefanis,[74a,74c] F. De Mori,[74a,74c] B. Ding,[66,1] X. X. Ding,[46,g] Y. Ding,[34] Y. Ding,[40] J. Dong,[1,58] L. Y. Dong,[1,63] M. Y. Dong,[1,58,63] X. Dong,[76] M. C. Du,[1] S. X. Du,[80] Z. H. Duan,[42] P. Egorov,[36,a] Y. H. Fan,[45] J. Fang,[1,58] S. S. Fang,[1,63] W. X. Fang,[1] Y. Fang,[1] Y. Q. Fang,[1,58] R. Farinelli,[29a] L. Fava,[74b,74c] F. Feldbauer,[3] G. Felici,[28a] C. Q. Feng,[71,58] J. H. Feng,[59] Y. T. Feng,[71] K. Fischer,[69] M. Fritsch,[3] C. D. Fu,[1] J. L. Fu,[63] Y. W. Fu,[1] H. Gao,[63] Y. N. Gao,[46,g] Yang Gao,[71,58] S. Garbolino,[74c] I. Garzia,[29a,29b] P. T. Ge,[76] Z. W. Ge,[42] C. Geng,[59] E. M. Gersabeck,[67] A. Gilman,[69] K. Goetzen,[13] L. Gong,[40] W. X. Gong,[1,58] W. Gradl,[35] S. Gramigna,[29a,29b] M. Greco,[74a,74c] M. H. Gu,[1,58] Y. T. Gu,[15] C. Y. Guan,[1,63] Z. L. Guan,[22] A. Q. Guo,[31,63] L. B. Guo,[41] M. J. Guo,[50] R. P. Guo,[49] Y. P. Guo,[12,f] A. Guskov,[36,a] J. Gutierrez,[27] K. L. Han,[63] T. T. Han,[1] W. Y. Han,[39] X. Q. Hao,[19] F. A. Harris,[65] K. K. He,[55] K. L. He,[1,63] F. H. H. Heinsius,[3] C. H. Heinz,[35] Y. K. Heng,[1,58,63] C. Herold,[60] T. Holtmann,[3] P. C. Hong,[12,f] G. Y. Hou,[1,63] X. T. Hou,[1,63] Y. R. Hou,[63] Z. L. Hou,[1] B. Y. Hu,[59] H. M. Hu,[1,63] J. F. Hu,[56,i] T. Hu,[1,58,63] Y. Hu,[1] G. S. Huang,[71,58] K. X. Huang,[59] L. Q. Huang,[31,63] X. T. Huang,[50] Y. P. Huang,[1] T. Hussain,[73] N. Hüsken,[27,35] N. in der Wiesche,[68] M. Irshad,[71,58] J. Jackson,[27] S. Jaeger,[3] S. Janchiv,[32] J. H. Jeong,[10] Q. Ji,[1] Q. P. Ji,[19] X. B. Ji,[1,63] X. L. Ji,[1,58] Y. Y. Ji,[50] X. Q. Jia,[50] Z. K. Jia,[71,58] H. B. Jiang,[76] P. C. Jiang,[46,g] S. S. Jiang,[39] T. J. Jiang,[16] X. S. Jiang,[1,58,63] Y. Jiang,[63] J. B. Jiao,[50] Z. Jiao,[23] S. Jin,[42] Y. Jin,[66] M. Q. Jing,[1,63] X. M. Jing,[63] T. Johansson,[75] X. Kui,[1] S. Kabana,[33] N. Kalantar-Nayestanaki,[64] X. L. Kang,[9] X. S. Kang,[40] M. Kavatsyuk,[64] B. C. Ke,[80] V. Khachatryan,[27] A. Khoukaz,[68] R. Kiuchi,[1] O. B. Kolcu,[62a] B. Kopf,[3] M. Kuessner,[3] A. Kupsc,[44,75] W. Kühn,[37] J. J. Lane,[67] P. Larin,[18] L. Lavezzi,[74a,74c] T. T. Lei,[71,58] Z. H. Lei,[71,58] H. Leithoff,[35] M. Lellmann,[35] T. Lenz,[35] C. Li,[47] C. Li,[43] C. H. Li,[39] Cheng Li,[71,58] D. M. Li,[80] F. Li,[1,58] G. Li,[1] H. Li,[71,58] H. B. Li,[1,63] H. J. Li,[19] H. N. Li,[56,i] Hui Li,[43] J. R. Li,[61] J. S. Li,[59] J. W. Li,[50] Ke Li,[1] L. J. Li,[1,63] L. K. Li,[1] Lei Li,[48] M. H. Li,[43] P. R. Li,[38,k] Q. X. Li,[50] S. X. Li,[12] T. Li,[50] W. D. Li,[1,63] W. G. Li,[1] X. H. Li,[71,58] X. L. Li,[50] Xiaoyu Li,[1,63] Y. G. Li,[46,g] Z. J. Li,[59] Z. X. Li,[15] C. Liang,[42] H. Liang,[1,63] H. Liang,[71,58] Y. F. Liang,[54] Y. T. Liang,[31,63] G. R. Liao,[14] L. Z. Liao,[50] Y. P. Liao,[1,63] J. Libby,[26] A. Limphirat,[60] D. X. Lin,[31,63] T. Lin,[1] B. J. Liu,[1] B. X. Liu,[76] C. Liu,[34] C. X. Liu,[1] F. H. Liu,[53] Fang Liu,[1] Feng Liu,[6] G. M. Liu,[56,i] H. Liu,[38,j,k] H. B. Liu,[15] H. M. Liu,[1,63] Huanhuan Liu,[1] Huihui Liu,[21] J. B. Liu,[71,58] J. Y. Liu,[1,63] K. Liu,[38,j,k] K. Y. Liu,[40] Ke Liu,[22] L. Liu,[71,58] L. C. Liu,[43] Lu Liu,[43] M. H. Liu,[12,f] P. L. Liu,[1] Q. Liu,[63] S. B. Liu,[71,58] T. Liu,[12,f] W. K. Liu,[43] W. M. Liu,[71,58] X. Liu,[38,j,k] Y. Liu,[80] Y. Liu,[38,j,k] Y. B. Liu,[43] Z. A. Liu,[1,58,63] Z. Q. Liu,[50] X. C. Lou,[1,58,63] F. X. Lu,[59] H. J. Lu,[23] J. G. Lu,[1,58] X. L. Lu,[1] Y. Lu,[7] Y. P. Lu,[1,58] Z. H. Lu,[1,63] C. L. Luo,[41] M. X. Luo,[79] T. Luo,[12,f] X. L. Luo,[1,58] X. R. Lyu,[63] Y. F. Lyu,[43] F. C. Ma,[40] H. Ma,[78] H. L. Ma,[1] J. L. Ma,[1,63] L. L. Ma,[50] M. M. Ma,[1,63] Q. M. Ma,[1] R. Q. Ma,[1,63] X. Y. Ma,[1,58] Y. Ma,[46,g] Y. M. Ma,[31] F. E. Maas,[18] M. Maggiora,[74a,74c] S. Malde,[69] Q. A. Malik,[73] A. Mangoni,[28b] Y. J. Mao,[46,g] Z. P. Mao,[1] S. Marcello,[74a,74c] Z. X. Meng,[66] J. G. Messchendorp,[13,64] G. Mezzadri,[29a] H. Miao,[1,63] T. J. Min,[42] R. E. Mitchell,[27] X. H. Mo,[1,58,63] B. Moses,[27] N. Yu. Muchnoi,[4,b] J. Muskalla,[35] Y. Nefedov,[36] F. Nerling,[18,d] I. B. Nikolaev,[4,b] Z. Ning,[1,58] S. Nisar,[11,l] Q. L. Niu,[38,j,k] W. D. Niu,[55] Y. Niu,[50] S. L. Olsen,[63] Q. Ouyang,[1,58,63] S. Pacetti,[28b,28c] X. Pan,[55] Y. Pan,[57] A. Pathak,[34] P. Patteri,[28a] Y. P. Pei,[71,58] M. Pelizaeus,[3] H. P. Peng,[71,58] Y. Y. Peng,[38,j,k] K. Peters,[13,d] J. L. Ping,[41] R. G. Ping,[1,63] S. Plura,[35] V. Prasad,[33] F. Z. Qi,[1] H. Qi,[71,58] H. R. Qi,[61] M. Qi,[42] T. Y. Qi,[12,f] S. Qian,[1,58] W. B. Qian,[63] C. F. Qiao,[63] J. J. Qin,[72] L. Q. Qin,[14] X. S. Qin,[50] Z. H. Qin,[1,58] J. F. Qiu,[1] S. Q. Qu,[61] C. F. Redmer,[35] K. J. Ren,[39] A. Rivetti,[74c] M. Rolo,[74c] G. Rong,[1,63] Ch. Rosner,[18] S. N. Ruan,[43] N. Salone,[44] A. Sarantsev,[36,c] Y. Schelhaas,[35] K. Schoenning,[75] M. Scodeggio,[29a,29b] K. Y. Shan,[12,f] W. Shan,[24] X. Y. Shan,[71,58] J. F. Shangguan,[55] L. G. Shao,[1,63] M. Shao,[71,58] C. P. Shen,[12,f] H. F. Shen,[1,63] W. H. Shen,[63] X. Y. Shen,[1,63] B. A. Shi,[63] H. C. Shi,[71,58] J. L. Shi,[12] J. Y. Shi,[1] Q. Q. Shi,[55] R. S. Shi,[1,63] X. Shi,[1,58] J. J. Song,[19] T. Z. Song,[59] W. M. Song,[34,1] Y. J. Song,[12] S. Sosio,[74a,74c] S. Spataro,[74a,74c] F. Stieler,[35] Y. J. Su,[63] G. B. Sun,[76] G. X. Sun,[1] H. Sun,[63] H. K. Sun,[1] J. F. Sun,[19] K. Sun,[61] L. Sun,[76] S. S. Sun,[1,63] T. Sun,[51,e] W. Y. Sun,[34] Y. Sun,[9] Y. J. Sun,[71,58] Y. Z. Sun,[1] Z. T. Sun,[50] Y. X. Tan,[71,58] C. J. Tang,[54] G. Y. Tang,[1] J. Tang,[59] Y. A. Tang,[76] L. Y. Tao,[72] Q. T. Tao,[25,h] M. Tat,[69] J. X. Teng,[71,58] V. Thoren,[75] W. H. Tian,[52] W. H. Tian,[59] Y. Tian,[31,63] Z. F. Tian,[76] I. Uman,[62b] Y. Wan,[55] S. J. Wang,[50] B. Wang,[1] B. L. Wang,[63] Bo Wang,[71,58] C. W. Wang,[42] D. Y. Wang,[46,g] F. Wang,[72] H. J. Wang,[38,j,k] J. P. Wang,[50] K. Wang,[1,58]

L. L. Wang,[1] M. Wang,[50] Meng Wang,[1,63] N. Y. Wang,[63] S. Wang,[38,j,k] S. Wang,[12,f] T. Wang,[12,f] T. J. Wang,[43] W. Wang,[59] W. Wang,[72] W. P. Wang,[71,58] X. Wang,[46,g] X. F. Wang,[38,j,k] X. J. Wang,[39] X. L. Wang,[12,f] Y. Wang,[61] Y. D. Wang,[45] Y. F. Wang,[1,58,63] Y. L. Wang,[19] Y. N. Wang,[45] Y. Q. Wang,[1] Yaqian Wang,[17,1] Yi Wang,[61] Z. Wang,[1,58] Z. L. Wang,[72] Z. Y. Wang,[1,63] Ziyi Wang,[63] D. Wei,[70] D. H. Wei,[14] F. Weidner,[68] S. P. Wen,[1] C. W. Wenzel,[3] U. Wiedner,[3] G. Wilkinson,[69] M. Wolke,[75] L. Wollenberg,[3] C. Wu,[39] J. F. Wu,[1,8] L. H. Wu,[1] L. J. Wu,[1,63] X. Wu,[12,f] X. H. Wu,[34] Y. Wu,[71] Y. H. Wu,[55] Y. J. Wu,[31] Z. Wu,[1,58] L. Xia,[71,58] X. M. Xian,[39] T. Xiang,[46,g] D. Xiao,[38,j,k] G. Y. Xiao,[42] S. Y. Xiao,[1] Y. L. Xiao,[12,f] Z. J. Xiao,[41] C. Xie,[42] X. H. Xie,[46,g] Y. Xie,[50] Y. G. Xie,[1,58] Y. H. Xie,[6] Z. P. Xie,[71,58] T. Y. Xing,[1,63] C. F. Xu,[1,63] C. J. Xu,[59] G. F. Xu,[1] H. Y. Xu,[66] Q. J. Xu,[16] Q. N. Xu,[30] W. Xu,[1] W. L. Xu,[66] X. P. Xu,[55] Y. C. Xu,[77] Z. P. Xu,[42] Z. S. Xu,[63] F. Yan,[12,f] L. Yan,[12,f] W. B. Yan,[71,58] W. C. Yan,[80] X. Q. Yan,[1] H. J. Yang,[51,e] H. L. Yang,[34] H. X. Yang,[1] Tao Yang,[1] Y. Yang,[12,f] Y. F. Yang,[43] Y. X. Yang,[1,63] Yifan Yang,[1,63] Z. W. Yang,[38,j,k] Z. P. Yao,[50] M. Ye,[1,58] M. H. Ye,[8] J. H. Yin,[1] Z. Y. You,[59] B. X. Yu,[1,58,63] C. X. Yu,[43] G. Yu,[1,63] J. S. Yu,[25,h] T. Yu,[72] X. D. Yu,[46,g] C. Z. Yuan,[1,63] L. Yuan,[2] S. C. Yuan,[1] Y. Yuan,[1,63] Z. Y. Yuan,[59] C. X. Yue,[39] A. A. Zafar,[73] F. R. Zeng,[50] S. H. Zeng,[72] X. Zeng,[12,f] Y. Zeng,[25,h] Y. J. Zeng,[1,63] X. Y. Zhai,[34] Y. C. Zhai,[50] Y. H. Zhan,[59] A. Q. Zhang,[1,63] B. L. Zhang,[1,63] B. X. Zhang,[1] D. H. Zhang,[43] G. Y. Zhang,[19] H. Zhang,[71] H. C. Zhang,[1,58,63] H. H. Zhang,[59] H. H. Zhang,[34] H. Q. Zhang,[1,58,63] H. Y. Zhang,[1,58] J. Zhang,[59] J. Zhang,[80] J. J. Zhang,[52] J. L. Zhang,[20] J. Q. Zhang,[41] J. W. Zhang,[1,58,63] J. X. Zhang,[38,j,k] J. Y. Zhang,[1] J. Z. Zhang,[1,63] Jianyu Zhang,[63] L. M. Zhang,[61] L. Q. Zhang,[59] Lei Zhang,[42] P. Zhang,[1,63] Q. Y. Zhang,[39,80] Shuihan Zhang,[1,63] Shulei Zhang,[25,h] X. D. Zhang,[45] X. M. Zhang,[1] X. Y. Zhang,[50] Y. Zhang,[69] Y. Zhang,[72] Y. T. Zhang,[80] Y. H. Zhang,[1,58] Yan Zhang,[71,58] Yao Zhang,[1] Z. D. Zhang,[1] Z. H. Zhang,[1] Z. L. Zhang,[34] Z. Y. Zhang,[76] Z. Y. Zhang,[43] G. Zhao,[1] J. Y. Zhao,[1,63] J. Z. Zhao,[1,58] Lei Zhao,[71,58] Ling Zhao,[1] M. G. Zhao,[43] R. P. Zhao,[63] S. J. Zhao,[80] Y. B. Zhao,[1,58] Y. X. Zhao,[31,63] Z. G. Zhao,[71,58] A. Zhemchugov,[36,a] B. Zheng,[72] J. P. Zheng,[1,58] W. J. Zheng,[1,63] Y. H. Zheng,[63] B. Zhong,[41] X. Zhong,[59] H. Zhou,[50] L. P. Zhou,[1,63] X. Zhou,[76] X. K. Zhou,[6] X. R. Zhou,[71,58] X. Y. Zhou,[39] Y. Z. Zhou,[12,f] J. Zhu,[43] K. Zhu,[1] K. J. Zhu,[1,58,63] L. Zhu,[34] L. X. Zhu,[63] S. H. Zhu,[70] S. Q. Zhu,[42] T. J. Zhu,[12,f] W. J. Zhu,[12,f] Y. C. Zhu,[71,58] Z. A. Zhu,[1,63] J. H. Zou,[1] and J. Zu[71,58]

(BESIII Collaboration)

[1]*Institute of High Energy Physics, Beijing 100049, People's Republic of China*
[2]*Beihang University, Beijing 100191, People's Republic of China*
[3]*Bochum Ruhr-University, D-44780 Bochum, Germany*
[4]*Budker Institute of Nuclear Physics SB RAS (BINP), Novosibirsk 630090, Russia*
[5]*Carnegie Mellon University, Pittsburgh, Pennsylvania 15213, USA*
[6]*Central China Normal University, Wuhan 430079, People's Republic of China*
[7]*Central South University, Changsha 410083, People's Republic of China*
[8]*China Center of Advanced Science and Technology, Beijing 100190, People's Republic of China*
[9]*China University of Geosciences, Wuhan 430074, People's Republic of China*
[10]*Chung-Ang University, Seoul, 06974, Republic of Korea*
[11]*COMSATS University Islamabad, Lahore Campus, Defence Road, Off Raiwind Road, 54000 Lahore, Pakistan*
[12]*Fudan University, Shanghai 200433, People's Republic of China*
[13]*GSI Helmholtzcentre for Heavy Ion Research GmbH, D-64291 Darmstadt, Germany*
[14]*Guangxi Normal University, Guilin 541004, People's Republic of China*
[15]*Guangxi University, Nanning 530004, People's Republic of China*
[16]*Hangzhou Normal University, Hangzhou 310036, People's Republic of China*
[17]*Hebei University, Baoding 071002, People's Republic of China*
[18]*Helmholtz Institute Mainz, Staudinger Weg 18, D-55099 Mainz, Germany*
[19]*Henan Normal University, Xinxiang 453007, People's Republic of China*
[20]*Henan University, Kaifeng 475004, People's Republic of China*
[21]*Henan University of Science and Technology, Luoyang 471003, People's Republic of China*
[22]*Henan University of Technology, Zhengzhou 450001, People's Republic of China*
[23]*Huangshan College, Huangshan 245000, People's Republic of China*
[24]*Hunan Normal University, Changsha 410081, People's Republic of China*
[25]*Hunan University, Changsha 410082, People's Republic of China*
[26]*Indian Institute of Technology Madras, Chennai 600036, India*
[27]*Indiana University, Bloomington, Indiana 47405, USA*

[28a]*INFN Laboratori Nazionali di Frascati, INFN Laboratori Nazionali di Frascati, I-00044 Frascati, Italy*
[28b]*INFN Sezione di Perugia, I-06100, Perugia, Italy*
[28c]*University of Perugia, I-06100, Perugia, Italy*
[29a]*INFN Sezione di Ferrara, INFN Sezione di Ferrara, I-44122 Ferrara, Italy*
[29b]*University of Ferrara, I-44122 Ferrara, Italy*
[30]*Inner Mongolia University, Hohhot 010021, People's Republic of China*
[31]*Institute of Modern Physics, Lanzhou 730000, People's Republic of China*
[32]*Institute of Physics and Technology, Peace Avenue 54B, Ulaanbaatar 13330, Mongolia*
[33]*Instituto de Alta Investigación, Universidad de Tarapacá, Casilla 7D, Arica 1000000, Chile*
[34]*Jilin University, Changchun 130012, People's Republic of China*
[35]*Johannes Gutenberg University of Mainz, Johann-Joachim-Becher-Weg 45, D-55099 Mainz, Germany*
[36]*Joint Institute for Nuclear Research, 141980 Dubna, Moscow region, Russia*
[37]*Justus-Liebig-Universitaet Giessen, II. Physikalisches Institut, Heinrich-Buff-Ring 16, D-35392 Giessen, Germany*
[38]*Lanzhou University, Lanzhou 730000, People's Republic of China*
[39]*Liaoning Normal University, Dalian 116029, People's Republic of China*
[40]*Liaoning University, Shenyang 110036, People's Republic of China*
[41]*Nanjing Normal University, Nanjing 210023, People's Republic of China*
[42]*Nanjing University, Nanjing 210093, People's Republic of China*
[43]*Nankai University, Tianjin 300071, People's Republic of China*
[44]*National Centre for Nuclear Research, Warsaw 02-093, Poland*
[45]*North China Electric Power University, Beijing 102206, People's Republic of China*
[46]*Peking University, Beijing 100871, People's Republic of China*
[47]*Qufu Normal University, Qufu 273165, People's Republic of China*
[48]*Renmin University of China, Beijing 100872, People's Republic of China*
[49]*Shandong Normal University, Jinan 250014, People's Republic of China*
[50]*Shandong University, Jinan 250100, People's Republic of China*
[51]*Shanghai Jiao Tong University, Shanghai 200240, People's Republic of China*
[52]*Shanxi Normal University, Linfen 041004, People's Republic of China*
[53]*Shanxi University, Taiyuan 030006, People's Republic of China*
[54]*Sichuan University, Chengdu 610064, People's Republic of China*
[55]*Soochow University, Suzhou 215006, People's Republic of China*
[56]*South China Normal University, Guangzhou 510006, People's Republic of China*
[57]*Southeast University, Nanjing 211100, People's Republic of China*
[58]*State Key Laboratory of Particle Detection and Electronics, Beijing 100049, Hefei 230026, People's Republic of China*
[59]*Sun Yat-Sen University, Guangzhou 510275, People's Republic of China*
[60]*Suranaree University of Technology, University Avenue 111, Nakhon Ratchasima 30000, Thailand*
[61]*Tsinghua University, Beijing 100084, People's Republic of China*
[62a]*Turkish Accelerator Center Particle Factory Group, Istinye University, 34010, Istanbul, Turkey*
[62b]*Near East University, Nicosia, North Cyprus, 99138, Mersin 10, Turkey*
[63]*University of Chinese Academy of Sciences, Beijing 100049, People's Republic of China*
[64]*University of Groningen, NL-9747 AA Groningen, The Netherlands*
[65]*University of Hawaii, Honolulu, Hawaii 96822, USA*
[66]*University of Jinan, Jinan 250022, People's Republic of China*
[67]*University of Manchester, Oxford Road, Manchester, M13 9PL, United Kingdom*
[68]*University of Muenster, Wilhelm-Klemm-Strasse 9, 48149 Muenster, Germany*
[69]*University of Oxford, Keble Road, Oxford OX13RH, United Kingdom*
[70]*University of Science and Technology Liaoning, Anshan 114051, People's Republic of China*
[71]*University of Science and Technology of China, Hefei 230026, People's Republic of China*
[72]*University of South China, Hengyang 421001, People's Republic of China*
[73]*University of the Punjab, Lahore-54590, Pakistan*
[74a]*University of Turin and INFN, University of Turin, I-10125 Turin, Italy*
[74b]*University of Eastern Piedmont, I-15121 Alessandria, Italy*
[74c]*INFN, I-10125 Turin, Italy*
[75]*Uppsala University, Box 516, SE-75120 Uppsala, Sweden*
[76]*Wuhan University, Wuhan 430072, People's Republic of China*
[77]*Yantai University, Yantai 264005, People's Republic of China*
[78]*Yunnan University, Kunming 650500, People's Republic of China*
[79]*Zhejiang University, Hangzhou 310027, People's Republic of China*
[80]*Zhengzhou University, Zhengzhou 450001, People's Republic of China*

[a]Also at the Moscow Institute of Physics and Technology, Moscow 141700, Russia.
[b]Also at the Novosibirsk State University, Novosibirsk, 630090, Russia.
[c]Also at the NRC "Kurchatov Institute", PNPI, 188300, Gatchina, Russia.
[d]Also at Goethe University Frankfurt, 60323 Frankfurt am Main, Germany.
[e]Also at Key Laboratory for Particle Physics, Astrophysics and Cosmology, Ministry of Education; Shanghai Key Laboratory for Particle Physics and Cosmology; Institute of Nuclear and Particle Physics, Shanghai 200240, People's Republic of China.
[f]Also at Key Laboratory of Nuclear Physics and Ion-beam Application (MOE) and Institute of Modern Physics, Fudan University, Shanghai 200443, People's Republic of China.
[g]Also at State Key Laboratory of Nuclear Physics and Technology, Peking University, Beijing 100871, People's Republic of China.
[h]Also at School of Physics and Electronics, Hunan University, Changsha 410082, China.
[i]Also at Guangdong Provincial Key Laboratory of Nuclear Science, Institute of Quantum Matter, South China Normal University, Guangzhou 510006, China.
[j]Also at MOE Frontiers Science Center for Rare Isotopes, Lanzhou University, Lanzhou 730000, People's Republic of China.
[k]Also at Lanzhou Center for Theoretical Physics, Lanzhou University, Lanzhou 730000, People's Republic of China.
[l]Also at the Department of Mathematical Sciences, IBA, Karachi 75270, Pakistan.